Drude weight increase by orbital and repulsive interactions in fermionic ladders

Andreas Haller,[1] Matteo Rizzi,[2,3] and Michele Filippone[4]

[1]*Institute of Physics, Johannes Gutenberg University, D-55099 Mainz, Germany*

[2]*Institute of Quantum Control (PGI-8), Forschungszentrum Jülich, D-52425 Jülich, Germany*

[3]*Institute for Theoretical Physics, University of Cologne, D-50937 Köln, Germany*

[4]*Department of Quantum Matter Physics, Ecole de Physique University of Geneva, Quai Ernest-Ansermet 24, CH-1211 Geneva 4, Switzerland*

(Received 29 November 2019; revised manuscript received 10 March 2020; accepted 11 March 2020; published 20 April 2020)

In strictly one-dimensional systems, repulsive interactions tend to reduce particle mobility on a lattice. Therefore, the Drude weight, controlling the divergence at zero-frequency of optical conductivities in perfect conductors, is lower than in noninteracting cases. We show that this is not the case when extending to quasi-one-dimensional ladder systems. Relying on bosonization, perturbative and matrix product states (MPS) calculations, we show that nearest-neighbor interactions and magnetic fluxes provide a bias between back- and forward-scattering processes, leading to linear corrections to the Drude weight in the interaction strength. As a consequence, Drude weights counterintuitively increase (decrease) with repulsive (attractive) interactions. Our findings are relevant for the efficient tuning of Drude weights in the framework of ultracold atoms trapped in optical lattices and equally affect topological edge states in condensed matter systems.

DOI: 10.1103/PhysRevResearch.2.023058

I. INTRODUCTION

The seminal work by Kohn [1] established the Drude weight as a crucial quantity to describe the conduction properties of strongly correlated quantum systems. At zero temperature ($T \to 0$), it weights the zero-frequency divergence of the conductivity [2–5]

$$\mathrm{Re}[\sigma(\omega)] = \mathcal{D}\delta(\omega) + \sigma_{\mathrm{reg}}(\omega), \tag{1}$$

signaling a perfect conductor, which, as conventional superconductors, supports nondissipative/ballistic transport. In quasi-one-dimensional conducting rings of size L, the Drude weight also determines the dissipationless persistent current $J = \mathcal{D}\Phi/L$ [6–14] generated in response to a (infinitesimal) magnetic flux Φ threading the ring. Persistent currents are an equilibrium property of quantum coherent conductors and are a phase-coherent manifestation of the Aharonov-Bohm (AB) phase Φ acquired by particles upon looping around the ring, equivalent to a twist in the periodic boundary condition. In consequence, Drude weights coincide with the susceptibility of the ground-state energy E to such a twist:

$$\mathcal{D} = L\pi \left.\frac{\partial^2 E}{\partial \Phi^2}\right|_{\Phi\to 0}. \tag{2}$$

In conducting systems, the Drude weight remains finite in the thermodynamic limit, while its exponential suppression signals insulating behavior. Beyond its usefulness for analytical and numerical calculations, Eqs. (1) and (2) establish a remarkable connection between the transport properties and the sensitivity to modified boundaries of quantum-coherent systems, underpinning, for instance, the scaling theory of Anderson localization [15–19] and many-body generalizations thereof [20–22].

The rich behavior displayed by Drude weights in the presence of interactions has important consequences for various quantum transport phenomena. Quantitative evaluation of Drude weights is important for the correct interpretation of experiments addressing related persistent currents in metallic rings [12–14,23]. Additionally, the divergent contribution in Eq. (1) does not always disappear at finite temperature in fine-tuned integrable models [24–36], and is also well described in real spin chains [37–44]. Drude weights also contribute to the Hall response of quasi-one-dimensional ladder systems [45,46].

Importantly, synthetic quantum matter systems, such as ultracold atoms confined in ring-shaped optical traps [47–55] provide an experimental platform to study orbital responses to an applied flux in which temperature, particle statistics, and even interactions can be engineered almost at will. Moreover, the currents driven by either displacing the confining potential [56] or tilting the system [57] reproduce those generated persistently by a flux Φ penetrating a ring geometry in an adiabatic approximation [46], therefore accessing Drude weights with open boundary conditions.

It is thus important, both on the experimental and fundamental level, to understand and develop physical intuition concerning the effects of strong correlations on the Drude weight. It is commonly believed that repulsive interactions reduce particle mobility in a many-body system, leading to a generic reduction of the Drude weight [19,58–60].

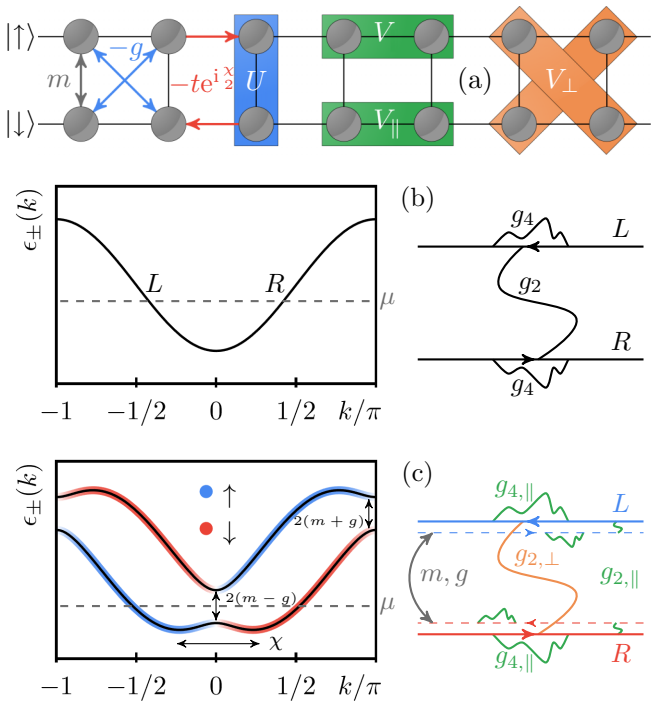

FIG. 1. (a) The interacting Creutz model, Eqs. (7)–(10). We represent interactions by colored boxes and tight-binding hopping elements as arrows connecting different lattice sites. (b) depicts the usual one-dimensional case. A single pair of distinct left and right movers is identified close to the chemical potential μ and $V_\parallel$ induces $g_{2/4}$ interaction processes that exactly compensate each other on the lattice. (c) illustrates the two-leg ladder case with magnetic flux ($g = 0$ for simplicity). A finite interchain hopping of amplitude m gaps out only one pair among the right or left movers of each singular chain (dashed lines), leading to a suppression of backscattering $g_{2,\parallel}$ processes compared to forward scattering $g_{4,\parallel}$ processes caused by $V_\parallel$. As a consequence, the Drude weight increases. We also sketch how $V_\perp$ increases backscattering, opposite to the action of $V_\parallel$.

Nevertheless, it was recently observed that this fact is remarkably violated in Creutz ladders [61]: the effect was attributed to the presence of an isolated Dirac cone in analogy to the anomalous magnetic orbital response of two-dimensional (2D) graphene [62].

In this work, we show that the increase of Drude weight by local repulsive interactions at zero temperature is actually a more general feature of quasi-1D interacting systems thread by a transverse magnetic flux χ, see Fig. 1. To demonstrate it's generality we rely on perturbative calculations, which are in perfect agreement with matrix product states (MPS) simulations. A more fundamental understanding is derived from the effective low-energy Luttinger liquid theory of interacting quantum ladders, showing that nearest-neighbor interactions and magnetic fluxes provide a bias between back- and forward-scattering processes. Finally, we connect this phenomenon with the quantum Hall effect [63], in which the presence of magnetic fluxes leads to the suppression of interaction-induced backscattering. In consequence, the prominence of forward-scattering on polarized edge states leads to increased mobility, as signaled by an increased Drude weight.

Remarkably, such Drude weight corrections are linear in the interaction strength, thus allowing for efficient tunability of this quantity by switching to attractive interactions, in which case the Drude weight is suppressed. Our findings are important as they shed new light on the transport properties of strongly correlated systems with nontrivial topological properties, which may be accessed both in synthetic and solid-state quantum matter systems.

The work is structured as follows: To fully appreciate our key results presented in Secs. IV and V, in Sec. II we review why repulsive density-density interactions do not yield a strong (i.e., linear in the interaction strength) renormalization of the Drude weight in strictly one-dimensional systems. Section III reviews the single-particle properties and band structure of the Creutz model. In Sec. IV, we calculate the leading-order corrections to the Drude weight in the interaction strength with standard perturbation theory, showing strong corrections to the Drude weight in excellent quantitative agreement to MPS simulations. Section V presents the effective Luttinger liquid interpretation of the Drude weight increase, showing bias between back- and forward-scattering processes induced by orbital effects and we conclude by making an important and novel connection to quantum Hall phases in two dimensions.

II. WEAK DRUDE WEIGHT RENORMALIZATION IN ONE DIMENSION

In strictly one dimension, interactions cannot possibly affect the Drude weight in Galilean invariant systems, due to the perfect decoupling of the center-of-mass motion (affected then by the flux insertion) from the internal degrees of freedom (affected instead by interactions). Noticeably, this holds true also for multicomponent systems, as long as the only coupling between different species is of density-density nature: in that case, it will be the total current (and therefore the total Drude weight) to be untouched by interactions, while off-diagonal drag coefficients may depend on the interspecies interaction strength. The presence of a lattice, once away from commensurate effects, which might resonate and open a gap, is expected to affect this important result only beyond leading order. These facts are readily understood in the bosonization formalism [64], which will later help us to clarify where the hack in the ladder case resides.

Consider a generic single-band tight-binding Hamiltonian, $\mathcal{H}_{\rm kin} = \sum_k \varepsilon(k) n_k$, in which $\varepsilon(k)$ is the band dispersion and n_k the density at momentum k. In a low-energy approximation, the band dispersion $\varepsilon(k)$ can be linearized close to the Fermi points, $\varepsilon(k) \sim \varepsilon(\pm k_{\rm F}) \pm v_{\rm F}(k \mp k_{\rm F})$, with $v_{\rm F}$ the Fermi velocity. Such a linearization allows to define two separate right- and left-moving fermions (R_j/L_j) out of the original fermions on lattice site j, $c_j \sim e^{ik_{\rm F}j} R_j + e^{-ik_{\rm F}j} L_j$, and their densities $n_{\alpha,i} = \alpha_i^\dagger \alpha_i$ ($\alpha = R, L$). In such Tomonaga-Luttinger-Dirac approximations, the fermionic fields can in turn be expressed via a pair of canonically conjugate bosonic fields ϕ and θ, $[\phi(x), \partial_{x'}\theta(x')] = i\pi\delta(x - x')$, which describe density and current fluctuations of the effective low-energy system: $n_i = n_{R,i} + n_{L,i} = -\partial_x \phi(x)/\pi$ and $J_i/v_{\rm F} = n_{R,i} - n_{L,i} = \partial_x \theta(x)/\pi$, respectively. The

Hamiltonian can be then exactly cast in the bosonized form $\mathcal{H}_{\rm kin} = \int \frac{dx}{2\pi} v_{\rm F}[(\partial_x\theta(x))^2 + (\partial_x\phi(x))^2]$ [64,65].

In the presence of (short-range) interactions, described by the Hamiltonian $\mathcal{H}_{\rm int} = \sum_{i,j} V_{i,j} n_i n_j$, the Luttinger liquid Hamiltonian is only slightly modified to

$$\mathcal{H}_{\rm LL} = \int \frac{dx}{2\pi}\Big[uK(\partial_x\theta(x))^2 + \frac{u}{K}(\partial_x\phi(x))^2\Big] + \mathcal{V}[\phi], \quad (3)$$

in which the Luttinger parameters u and K correspond to the velocity of the collective plasma oscillation of the gas and give information about interactions, respectively: e.g., repulsive 1D fermions are usually described by $K \leqslant 1$. The additional term $\mathcal{V}[\phi]$ collects all additional nonquadratic terms generated by density-density interactions, which, importantly, do not depend on the bosonic operator θ, be the system on a lattice or not: indeed, the definition of the current operator obtained via the continuity equation is unaffected,

$$\begin{aligned}[n, \mathcal{H}_{\rm int}] = 0 \;\Rightarrow\; \partial_x J = -\partial_t n = -i[n, \mathcal{H}] = -i[n, \mathcal{H}_{\rm kin}] \\ = i[\partial_x\phi, \mathcal{H}_{\rm kin}]/\pi = v_{\rm F}\partial_x^2\theta/\pi. \end{aligned} \quad (4)$$

As a crucial consequence, the product uK, i.e., the Drude weight, remains equal to the noninteracting Fermi velocity $v_{\rm F}$, unaffected by interactions. Standard minimal coupling, in which threading a flux Φ in a ring geometry is equivalent to shift momenta as $k \to k - \Phi/L$ [i.e., here $\partial_x\theta(x) \to \partial_x\theta(x) - \Phi/L$], combined with Eqs. (2) and (3), leads to

$$\mathcal{D} = uK = \mathcal{D}_0 = v_{\rm F}. \quad (5)$$

In the absence of commensurability effects or other gap-formation mechanisms, the corrections $\mathcal{V}[\phi]$ are usually irrelevant in the renormalization group sense [64], and therefore they do not affect the validity of the Hamiltonian (3) but at most lead to a renormalization of the Luttinger liquid parameters $(u, K) \to (u^*, K^*)$. The Drude weight gets renormalized $\mathcal{D}_0 = v_{\rm F} \to \mathcal{D}^* = u^*K^*$ as well, but, crucially for the following discussion, such renormalization is usually weak (i.e., at most of order V^2 in the perturbative expansion) and the Drude weight is suppressed $\mathcal{D}^* < \mathcal{D}_0$ [19,58,59].

Alternatively, as we are going to rederive in the following, the validity of the identity (5) is also understood from the fact that interactions generate coupling between left and right movers, so-called g_2 backscattering processes: $g_2 n_R n_L$; and right/left movers themselves, the so-called g_4 forward-scattering processes: $g_4(n_R n_R + n_L n_L)/2$. The Drude weight is affected by them as follows [64]:

$$\mathcal{D} = \mathcal{D}_0 + \frac{g_4 - g_2}{2\pi}. \quad (6)$$

For the same reasons leading to Eq. (5), in conventional lattice systems one always finds $g_4 = g_2$ and thus no renormalization of the Drude weight occurs to leading order in the interactions.

The arguments leading to the identity (5), namely the commutation rule (4), do not generally apply in the presence of orbital effects in quasi-1D systems and, in this paper, we show a very simple mechanism leading to a modification of the Drude weight in quantum ladders, which is linear in the interaction amplitudes and, remarkably, is positive in presence of typical intrachain repulsive terms.

III. MODEL

The reference system and a sketch of the physical processes at work are illustrated in Fig. 1. As an illustration, we consider a two-leg ladder of fermions (labeled as $\uparrow$ and $\downarrow$ species) where the plaquettes are threaded by a magnetic flux χ. The generalization to the case with N legs, relevant for topologically protected quantum Hall regimes, is discussed in Appendix C, with similar conclusions. For the kinetic/noninteracting part of the full Hamiltonian, we consider the following:

$$\mathcal{H}_{\rm kin} = \frac{1}{2}\sum_{j=1}^{L} c_j^\dagger\big(\big(-te^{i\frac{\chi}{2}\sigma_z} - g\sigma_x\big)c_{j-1} + m\sigma_x c_j\big) + \text{H.c.}, \quad (7)$$

in which we assume periodic boundary conditions $c_0 = c_L$, define the fermionic annihilation operators $c_j = (c_{j\uparrow}, c_{j\downarrow})^T$ and express the tight-binding Hamiltonian using the Pauli matrices σ_x, σ_y, and σ_z. In the two-leg case, the Hamiltonian (7) also describes spinful one-dimensional fermions in which χ is a Rashba spin-orbit coupling [66–69]. Otherwise, Eq. (7) generally describes spinless fermions on a ladder, in which σ is the leg index, which can assume more than two values to describe systems with synthetic dimensions [56,57,70]. Equivalently, it describes two-dimensional lattices of spinless fermions in which σ labels the lattice position in the second dimension, a case, which is explicitly addressed in Appendix C. For $m \neq 0$, $g = 0$ and generic values of χ, this represents the minimal instance of a quasi-1D system pierced by magnetic flux, which has been extensively investigated under various aspects [67,71–77], but interestingly not the one addressed here. For $\chi = \pi$ and $g \neq 0$, the model is the Creutz ladder [78,79], at whose fine-tuned point $m = g = t$ the anomalous behavior of the Drude weight was originally pointed out and attributed to the presence of an isolated Dirac cone [61]. In this work, we go beyond the fine-tuned point studied in Ref. [61] and consider a much wider class of tight-binding models compatible with Eq. (7).

On top of the tight-binding part $\mathcal{H}_{\rm kin}$, we dress the lattice with orbital-selective density-density interactions $\mathcal{H}_{\rm int} = \mathcal{H}_\parallel + \mathcal{H}_\perp + \mathcal{H}_U$. Our main focus will be on intrachain (parallel) nearest-neighbors interactions

$$\mathcal{H}_\parallel = V_\parallel \sum_j (n_{j,\uparrow}n_{j+1,\uparrow} + n_{j+1,\downarrow}n_{j,\downarrow}), \quad (8)$$

but, motivated by recent experiments achieving orbital effects with synthetic dimensions [56,57], we will also consider nearest-neighbor (perpendicular) and $SU(2)$ symmetric on-site repulsion between different legs

$$\mathcal{H}_\perp = V_\perp \sum_j (n_{j,\uparrow}n_{j+1,\downarrow} + n_{j+1,\downarrow}n_{j,\uparrow}), \quad (9)$$

$$\mathcal{H}_U = U \sum_j n_{j,\uparrow}n_{j,\downarrow}. \quad (10)$$

Before considering the effect of interactions on the Drude weight, we discuss first the band spectrum of the noninteracting model (7), which in Fourier k space reads

$$\mathcal{H}_{\rm kin} = \sum_k c_k^\dagger H_0(k) c_k, \quad H_0(k) = h_0(k)\mathbb{1} + \vec{h}(k)\cdot\vec{\sigma}, \quad (11)$$

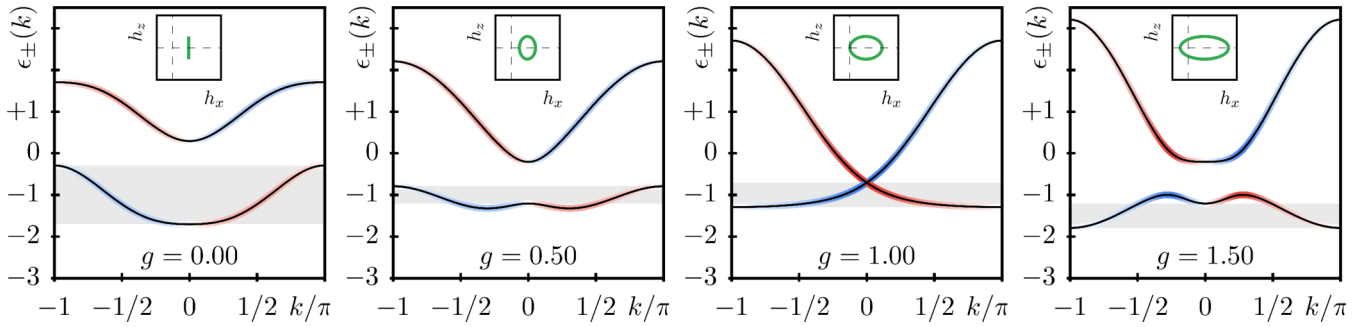

FIG. 2. Spin components of the bands for different parameters g, χ as displayed at the top of the figures; we fix $m = t = 1$ and $\chi = \pi/2$ for simplicity. Black lines mark the band dispersion and the color represents the band polarization along the canonical axis ($\uparrow$ in blue, $\downarrow$ in red). White implies a perfect superposition of $\uparrow$ and $\downarrow$ species. The green inset circle represents the winding of $\vec{h}(k)$ and dashed axes mark the origin. The gray region marks chemical potentials to fix a central charge $c = 1$ with a single left and right mover at $\pm k_F$, the starting point of the bosonization approach exploited in Sec. V.

where $\vec{h} = (h_x, h_y, h_z)$ and $\vec{\sigma} = (\sigma_x, \sigma_y, \sigma_z)$. In the gauge chosen above,

$$h_0 = -t\cos(k)\cos\left(\frac{\chi}{2}\right), \qquad h_x = m - g\cos(k), \tag{12}$$

$$h_y = 0, \qquad h_z = t\sin(k)\sin\left(\frac{\chi}{2}\right), \tag{13}$$

which is readily put in the diagonal form $\mathcal{H}_{\rm kin} = \sum_{k,v=\pm} \varepsilon_v(k) d^\dagger_{v,k} d_{v,k}$ by the transformation $c_k = U(k) d_k$ with, for $h_y = 0$,

$$U(k) = \frac{1}{\sqrt{2}}\left(\mathbb{1}\cdot\sqrt{1+\frac{h_z}{h}} - i\,\mathrm{sgn}[h_x]\sigma_y\cdot\sqrt{1-\frac{h_z}{h}}\right), \tag{14}$$

leading to

$$\begin{pmatrix} c_{\uparrow,k} \\ c_{\downarrow,k} \end{pmatrix} = \begin{pmatrix} u(k) & -v(k) \\ v(k) & u(k) \end{pmatrix}\begin{pmatrix} d_{+,k} \\ d_{-,k} \end{pmatrix},$$
$$u = \frac{1}{\sqrt{2}}\sqrt{1+\tilde{h}_z}, \qquad v = \frac{\mathrm{sgn}[h_x]}{\sqrt{2}}\sqrt{1-\tilde{h}_z}, \tag{15}$$

with dispersion $\varepsilon_\pm(k) = h_0(k) \pm h(k)$, norm of the Bloch vector $h(k) = |\vec{h}(k)| = (h_x^2 + h_y^2 + h_z^2)^{-1/2}$ and $\tilde{h}_i = h_i/h$. This can be checked by verifying $U^\dagger(k) H_0(k) U(k) = h_0(k)\mathbb{1} + h(k)\sigma_z$. In Fig. 2, different spectra are given for different set of parameters of the Creutz model, among which the band dispersion sketched in Fig. 1 is reproduced. In the following sections, we will exploit heavily the two basic ingredients to obtain the strong renormalization of the Drude weight: (i) a transverse flux χ, which polarizes the dispersion bands along a chosen axis and (ii) a gapping mechanism such that only one pair of the chiral modes remains intact. As a consequence, the densities defined in the chosen axis (here, σ_z) are spread asymmetrically in k space (as depicted in Figs. 1–2) and same-spin density-density interactions favor forward-scattering, whereas different-spin density-density terms favor backscattering processes.

IV. PERTURBATION THEORY

As a supporting point for the Luttinger liquid analysis we develop in Sec. V, we first derive the corrections to the Drude weight relying on leading-order perturbation theory in the interaction strengths $V_\parallel$, $V_\perp$, and U.

The MPS simulations reported in Fig. 3 show that standard perturbation theory captures the corrections to the Drude weight, remarkably not suffering from the typical logarithmic divergences arising in perturbation theory predictions of many other quantities in one-dimensional systems. The appearance of such divergencies ultimately signals the breakdown of long-lived single-particle excitations, which are replaced by collective plasmonic excitations well described through bosonization. Still, the low-energy excitation spectrum itself is not suddenly changed through this breakdown as long as

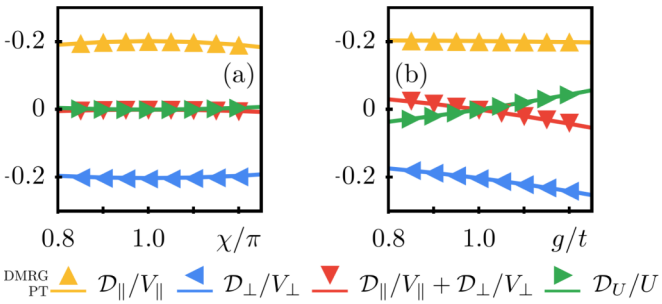

FIG. 3. Renormalization of the Drude weight by interaction (different colors and symbols). Continuous lines represent the thermodynamic limit of the perturbative calculation given in Eqs. (16), (18), (19) and symbols represent results obtained by MPS simulations. Numerical values are converged up to the third decimal digit. The system size is $N/L = 20/32$. Each set of data is obtained by the interplay of the kinetic term with individual interactions $\mathcal{H} = \mathcal{H}_{\rm kin} + \mathcal{H}_i$ with weak interaction amplitudes $V_\parallel = 0.1t$, $V_\perp = 0.1t$, $V_\parallel = V_\perp = 0.1t$, and $U = 0.125t$. The two figures demonstrate the robustness of the strong Drude weight renormalization, namely its increase for $V_\parallel > 0$ and decrease for $V_\perp > 0$ around the fine-tuned point of a single Dirac cone $m/t = g/t = \chi/\pi = 1$. Hereby, we devote our focus to the influence of the individual interactions by subtracting the corresponding noninteracting value $\mathcal{D}_0$ from the total susceptibility, i.e., $\mathcal{D}_i = \mathcal{D} - \mathcal{D}_0$. In (a) we display the interaction-induced Drude weight shift $\mathcal{D}_i$ versus transverse flux χ, in which the curvature of the two $SU(2)$ symmetric interactions denoted by red (down-triangle) and green (right triangle) is not visible in the chosen scaling. To quantify, the plotted values of D_U/U are all inside the interval $[0, 5] \times 10^{-3}$ and $\mathcal{D}_\perp/V_\perp + \mathcal{D}_\parallel/V_\parallel$ resides in $[-4.2, 0] \times 10^{-3}$. (b) shows $\mathcal{D}_i$ as a function of the nearest neighbor interspecies hopping amplitude g/t.

the interactions do not induce band gaps (e.g., Mott gaps at commensurate fillings [80]). As a consequence of the Drude weight being directly related to the ground-state energy, a perturbative expansion thereof does not suffer from the aforementioned divergent contributions away from interaction-induced band gap formations.

Equation (2) requires to derive first the corresponding corrections to the ground-state energy. We focus on the situation of interest, in which only the lowest band ε_- is occupied ($n_{+,k} = 0\,\forall k$). To leading order, the interaction-induced corrections to the Drude weight are obtained by averaging the interaction terms onto the ground state. A magnetic flux threading the ring is equivalent to twisting the boundary by a phase Φ and a matter of substituting $k \to k - \Phi/L$, upon which we expand to second order in Φ and then approach the thermodynamic limit $\frac{1}{L}\sum_k \to \frac{1}{2\pi}\int dk$. Exploiting the fact that $h_{x/z}$ is an even/odd function and the integral boundaries are all symmetric around $k = 0$ (after the Taylor expansion in the flux Φ), one finds

$$\langle \mathcal{H}_\parallel \rangle = \frac{V_\parallel L}{2}\left(n^2 - \left(\frac{H^{1,0}_{z,0}}{2\pi}\right)^2\right) + \frac{\Phi^2}{2\pi L}\mathcal{D}_\parallel,$$
$$\mathcal{D}_\parallel = \frac{V_\parallel}{4\pi}\left(H^{0,0^2}_{z,1} - H^{0,1^2}_{z,1} - H^{1,0}_{z,2}H^{1,0}_{z,0}\right) \tag{16}$$

with $n = N/L$ being the total density and we defined integral functions of the Bloch vector components $\tilde{h}_i$, which depend upon the Fermi sea (FS)

$$H^{\alpha,\beta}_{i,n} = \int_{FS}\left(\sin^\alpha(k)\cos^\beta(k)\frac{\partial^n}{\partial k^n}\tilde{h}_i(k)\right)dk. \tag{17}$$

The above and also all following expansions in the flux are actually correct up to $O(\Phi^4)$ since all odd orders are proportional to symmetric integrals of odd functions and thus vanish. The interspecies interaction returns

$$\langle \mathcal{H}_\perp \rangle = \frac{V_\perp L}{2}\left(n^2 - \left(\frac{H^{0,1}_{x,0}}{2\pi}\right)^2\right) + \frac{\Phi^2}{2\pi L}\mathcal{D}_\perp,$$
$$\mathcal{D}_\perp = -\frac{V_\perp}{4\pi}\left(H^{0,0^2}_{z,1} + H^{1,0^2}_{x,1} + H^{0,1}_{x,2}H^{0,1}_{x,0}\right) \tag{18}$$

and the on-site interaction results in

$$\langle \mathcal{H}_U \rangle = \frac{UL}{4}\left(n^2 - \left(\frac{H^{0,0}_{x,0}}{2\pi}\right)^2\right) + \frac{\Phi^2}{2\pi L}\mathcal{D}_U,$$
$$\mathcal{D}_U = -\frac{U}{8\pi}\left(H^{0,0^2}_{z,1} + H^{0,0}_{x,2}H^{0,0}_{x,0}\right). \tag{19}$$

The Drude renormalization by interaction, according to leading-order perturbation theory, depends on the precise form of the microscopic model and does not follow any universal law. Strikingly, if we restrict to a single pair of Fermi points, the Drude weight increases for $V_\parallel > 0$ and decreases for $V_\perp > 0$ throughout the entire phase space m, g, t, which can be readily checked by evaluating Eq. (16) and (18) (see Appendix A, Fig. 5). As a trivial consequence, but in contrast to the common intuition, attractive interactions ($V_\parallel < 0$) decrease the orbital response function $\mathcal{D}$. In case of absent transverse magnetic flux $\chi = 0$, there is no renormalization of the Drude weight. The reason for such absence of strong (linear in the interactions) renormalization is the absence of any symmetry breaking mechanism between g_4 and g_2 processes induced by interactions, which are triggered by a finite χ as exemplified in Fig. 1 based on the Luttinger liquid analysis we carry out in Sec. V. Moreover, we also notice that the remarkable strong absence of renormalization $\mathcal{D}_U = 0$ and $D_\parallel/V_\parallel + D_\perp/V_\perp = 0$ in leading-order perturbation theory initially derived in Ref. [61] does not hold in general, but applies only for very special points in the phase space such as the single Dirac cone setting at $m/t = g/t = \chi/\pi = 1$ [more generally, the particle-hole symmetric Dirac cone setting at $m/t = g/t = \sin(\chi/2)$]. Finally, we emphasize the perfect agreement between perturbative results and MPS simulations for a weakly interacting system of size $N/L = 20/32$ as presented in Fig. 3.

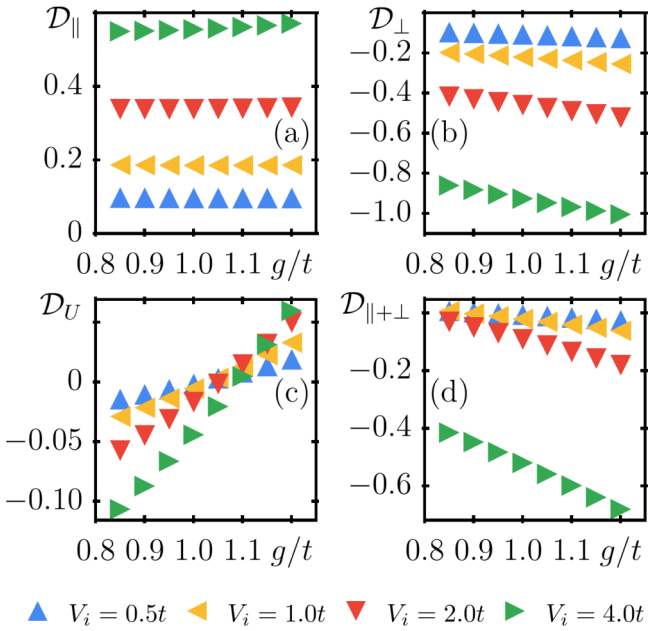

FIG. 4. Change of the Drude weight obtained by MPS simulations for different interaction amplitudes signalled by different colors and markers. The displayed values are converged up to the third decimal digit. The density of the system is $n = \frac{N}{L} = \frac{20}{32}$, $m/t = \chi/\pi = 1$, and g is relaxed to values around the topological transition at $g/t = 1$. (a) Drude increase induced by $\mathcal{H}_\parallel$ and (b) Drude decrease by $\mathcal{H}_\perp$. (c) Drude renormalization by $\mathcal{H}_U$ and (d) by $\mathcal{H}_\parallel + \mathcal{H}_\perp$ for the case $V_\parallel = V_\perp$. The effect is observed for any simulated amplitude of the interactions and irrespective of the underlying topology. Notice that the renormalization of the Drude weight due to $\mathcal{H}_\perp$ is stronger and very asymmetrical compared to $\mathcal{H}_\parallel$.

We also stress the fact that such corrections to the Drude weight are actually strong and can be comparable to the noninteracting value itself, as clearly shown by the MPS simulations reported in Fig. 4, in which we considered values of the interactions comparable with the parameters of the noninteracting model (7). The presented predictions from perturbation theory are qualitatively captured by the effective bosonized low-energy model, which we derive in the next section.

V. BOSONIZATION AND CONNECTION TO QUANTUM HALL SYSTEMS

The physical reason behind the linear increase and suppression of the Drude weight by the $V_\parallel$ and $V_\perp$ interaction, in the presence of a finite transverse flux χ, becomes apparent in the bosonization formalism. The bosonization of the interacting Creutz model requires a linearization of the spectrum close to the Fermi energy.

We consider the case of central charge $c = 1$ (i.e., two Fermi points) with the chemical potential crossing the lower band $\varepsilon_-(k)$. Even though we keep the discussion general here, the reader can think of the situations depicted in Fig. 2. Proceeding in analogy to Refs. [80–82], we approximate the two species of $\uparrow$ / $\downarrow$ fermions as a superposition of a single pair of left (L) and right (R) movers. Thus, the kinetic part of the Hamiltonian takes the form (3) with $v_\mathrm{F} = \partial_k \varepsilon_-(k)|_{k=k_\mathrm{F}}$. To bosonize the interactions, we switch to the continuum and apply the aforementioned transformation onto the spin-density operators to be inserted in $\mathcal{H}_\mathrm{int}$. We consider situations out of quarter-filling, in which umklapp terms $\propto e^{4ixk_\mathrm{F}} R^\dagger R^\dagger L L$ stop oscillating and may cause relevant gap-leading perturbations [81]. The total density operator thus becomes

$$n_i \sim n_R(x) + n_L(x) \\ -2u(k_\mathrm{F})v(-k_\mathrm{F})[e^{-2ik_\mathrm{F}x} R^\dagger(x) L(x) + \mathrm{H.c}]. \quad (20)$$

This density representation differs from that of a truly 1D spinless Luttinger liquid by the presence of the coherence factors u and v. At this stage it is possible to understand the reason why the relation (5), valid for strictly 1D systems, does not hold in our context: the projection via Eq. (15) on the low-energy sector captured by this bosonization approach is not a Bogoliubov transformation, as it does not preserve the fermionic anticommutation relations of the operators $c_{\uparrow/\downarrow}$. Moreover, it is responsible for the modification of the commutator with the interacting Hamiltonian, which becomes nonzero, $[n(x), \mathcal{H}_\mathrm{int}] \neq 0$. As we have already seen in Sec. II, such a condition is necessary not to modify the current operator and derive Eq. (5). Here, we explicitly lack this condition and expect thus a strong renormalization of the product uK for the effective Hamiltonian.

The mapping to the standard Luttinger liquid Hamiltonian (3) occurs via the usual bosonization identities $R(x) \sim e^{-i(\phi(x)-\theta(x))}$ and $L(x) \sim e^{i(\phi(x)+\theta(x))}$ [64]. The densities are given by $n_R(x) = [\partial_x\theta(x) - \partial_x\phi(x)]/2\pi$ and $n_L(x) = -[\partial_x\theta(x) + \partial_x\phi(x)]/2\pi$, which allows us to identify the bosonized Hamiltonian (3) with renormalized Luttinger parameters

$$\frac{uK}{v_\mathrm{F}} = 1 + \frac{1}{2\pi} \sum_{i\in\{\parallel,\perp,U\}} V_i(g_{4,i} - g_{2,i}), \quad (21)$$

$$\frac{u}{v_\mathrm{F}K} = 1 + \frac{1}{2\pi} \sum_{i\in\{\parallel,\perp,U\}} V_i(g_{4,i} + g_{2,i}), \quad (22)$$

for which the detailed derivation of the g factors is given in Appendix B and presented in Table I. The key result of this paper is resumed by the fact that

$$g_{4,\parallel} - g_{2,\parallel} = +2(u^2 - v^2)^2 = 2\tilde{h}_z(k_\mathrm{F})^2 > 0. \quad (23)$$

TABLE I. Renormalization of the Luttinger parameters in Eq. (21). The first column lists the different nearest-neighbor interactions and corresponding g_2 and g_4 factors.

V_i	$g_{4,i}$	$g_{2,i}$
$V_\parallel$	$2(u^4 + v^4) - 4u^2v^2\cos(2k_\mathrm{F})$	$g_{4,\perp}$
$V_\perp$	$4u^2v^2[1 - \cos(2k_\mathrm{F})]$	$g_{4,\parallel}$

As a consequence, in the presence of repulsive intrachain nearest-neighbor interactions, bosonization predicts the increase of the Drude weight by repulsive interactions.

Given the remarkable fact that such correction is linear in the interaction constant $V_\parallel$, attractive interactions reduce the mobility of such systems ($\mathcal{D} < \mathcal{D}_0$). Notice also that this result holds irrespective of the topological nature of the bands in the Creutz model ($m \lessgtr g$). The particular interest in the bosonization approach is that it allows us to readily identify the breaking of symmetry between the relevant forward- and backscattering processes (g_4 and g_2, respectively) responsible for such mobility increase in the presence of intrachain interactions. Notice further that, also within bosonization, no renormalization of the Drude weight occurs in the absence of transverse magnetic flux $\chi = 0$. As sketched in Fig. 1, the possibility to induce, via magnetic fluxes, orbital effects in such ladder system, allows us to suppress interaction-induced backscattering between left and right movers as these modes are separated in space (spin polarized).

Such a phenomenon can be put in connection to the exponential suppression of backscattering by topological bulk protection in quantum Hall systems [63]. As we discuss in detail by extending to the multileg case in Appendix C, following the spirit of the coupled-wire construction of topological insulators [83,84]. As modes in the bulk are gapped, local interactions cannot efficiently couple any degree of freedom to the chiral modes, which are localized at the sample edge, thus backscattering is exponentially suppressed with the number of legs. Nevertheless a residual effect of interactions remains, which is forward scattering, that, as made explicit by the bosonization formula (6), increases the Drude weight. In quantum Hall systems, which feature ballistic edges states at their border, the Drude weight is also expected to be renormalized by interactions [85,86]. Nevertheless, such corrections were never calculated explicitly in lattice models, especially not the increase induced by repulsive interactions discussed in this work. Our work predicts that, surprisingly, such renormalization is actually strong (linear) in the interaction strength and generally leads to an increase of the Drude weight for short-range repulsive interactions, in striking contrast to the one-dimensional limit.

Additionally, we notice that, in the bosonization formalism, introducing interchain interactions $V_\perp$ has exactly the opposite effect on the Drude weight, namely its suppression. In the quantum Hall picture discussed in the previous paragraph, the $\mathcal{H}_\perp$ interaction can be seen as a long-range interaction coupling left- and right-chiral edges. As a consequence, backscattering is induced and thus the Drude weight is reduced. However, this kind of long-range interaction is unlikely to occur in a typical condensed matter system. Nevertheless they (i.e., $\mathcal{H}_U$ interactions) are actually the ones mainly at

work in synthetic systems involving artificial gauge fields [56,57] and induce nontrivial effects [87], which deserve further investigation in the presence of orbital effects.

We conclude this section mentioning that the bosonization results are quantitatively different from the perturbation calculations reported in Sec. IV, on which we can fully rely given their perfect comparison with MPS calculations. Nevertheless the qualitative picture remains the same, apart from the perfect cancellation of the contributions resulting from $\mathcal{H}_\parallel + \mathcal{H}_\perp$. Such quantitative discrepancies are expected in bosonization given the strong approximation regarding the linearization of the dispersion and the presence of an underlying lattice in the microscopic model. In Appendix B, we explicitly address these discrepancies between bosonization and perturbation theory in detail.

Moreover, we mention that the renormalization of the Drude weight of the $SU(2)$ symmetric interaction $\mathcal{H}_U$ remains intriguing. In particular, Fig. 3(b) and Fig. 4(c) show an interesting change of sign as a function of g. Even though the perturbative prediction perfectly overlaps with all MPS simulations, we could not provide a more intuitive explanation of this feature relying on bosonization. The main difficulty here is related to the loss of information about the fact that operators are originally at the same point after rotating Eq. (7) to the diagonal basis. We leave the investigation of this issue for future work.

VI. DISCUSSION AND CONCLUSION

As mentioned in Sec. I, there is a strong experimental and fundamental interest in the coherent transport properties of correlated systems confined to ring geometries [47–55]. Knowledge about the behavior of the Drude weight in this context is crucial, as this quantity controls the magnitude of persistent currents in such systems, and also in their condensed matter analogs [6–14].

In particular, our results shed new light on an intriguing effect visible in such strongly correlated quantum systems: We demonstrated how repulsive (attractive) interactions counterintuitively increase (decrease) the mobility of interacting fermions in the presence of orbital effects. This phenomenon is strong in the sense that it depends linearly on the interaction strength, opposed to strictly one-dimensional systems. Additionally, our predictions are very general: we demonstrated that the counterintuitive renormalization is linked to the topological protection of edge states in the quantum Hall effect, in which the only possible effect for interactions is limited to forward-scattering.

We derived the effective continuum Luttinger liquid low-energy theory of the interacting Creutz model and focused on the situation with only two Fermi points, that is, central charge $c = 1$. We have shown that the Drude weight changes linearly in the coupling parameters $V_\parallel, V_\perp$ of the two orbital-selective nearest-neighbor interactions. Our study clarifies and generalizes the possibility of tuning the Drude weight observed in a previous study using MPS and second-order perturbation theory [61], predicting a linear dependence of the Drude weight with respect to $V_\parallel$, $V_\perp$, and U. In this work, we limited the bosonization approach to the simplest situation with only two Fermi points, but a generalization to higher central charges is straightforward. A direct comparison with leading-order perturbation theory and MPS simulations reveals quantitative shortcomings of the standard bosonization procedure regarding the prediction of transport properties. Future work in this direction should definitively address these issues.

Interesting perspectives concern the geometrical interpretation of the effects discussed in this work [88] and the study of the interplay of quantum impurities and bulk interactions in such systems [54,89]. Moreover, it is completely open for investigation how the interactions studied in this paper affect a setup in which energy and mass transport are induced by biased reservoirs [90–95]. In this case, interactions are not expected to affect the mass conductance [96], but only the thermal conductance, leading to the violation of the Wiedemann-Franz law [94]. In this setting, transport is controlled by conductances, rather than Drude weights and transverse magnetic fields in the connecting region are expected to lead novel quantized effects [97,98]. Another direction of interest concerns the renormalization of the transverse flux χ susceptibility, in order to stabilize end enhance pretopological fractional excitations [67,76,77,99].

ACKNOWLEDGMENTS

The authors thank C.-E. Bardyn, M. Burrello, P. van Dongen, T. Giamarchi, K. Le Hur, A. Minguzzi, S. Manmana, S. Paeckel, I. V. Protopopov, P. Schmoll, and I. Schneider for fruitful and inspiring discussions. A.H. is thankful for the financial support of the MAINZ Graduate School of Excellence and the Max Planck Graduate Center. M.R. and A.H. acknowledge support from the Deutsche Forschungsgesellschaft (DFG) through the grant OSCAR 277810020 (RI 2345/2-1). M.F. acknowledges support from the FNS/SNF Ambizione Grant PZ00P2_174038. The MPS simulations were run on the Mogon cluster of the Johannes Gutenberg-Universität (made available by the CSM and AHRP), with a code based on a flexible Abelian Symmetric Tensor Networks Library, developed in collaboration with the group of S. Montangero at the University of Ulm (now moved to Padua).

APPENDIX A: PERTURBATION THEORY: SUPPLEMENTARY

We start by giving the first-order correction of a generic density-density interaction of the form $\mathcal{H}_{\alpha,\beta,i} = V_{\alpha,\beta,i} \sum_j n_{\alpha,j} n_{\beta,j+i}$. According to the Wick-theorem, we expand its two-point correlator following the usual contraction rules

$$\begin{aligned}\mathcal{H}_{\alpha,\beta,i}/V_{\alpha,\beta,i} &= \sum_j \langle n_{\alpha,j} n_{\beta,j+i}\rangle = \sum_j \langle c^\dagger_{\alpha,j} c_{\alpha,j} c^\dagger_{\beta,j+i} c_{\beta,j+i}\rangle \\ &= \frac{1}{L}\sum_{k,l} (\langle n_{\alpha,k}\rangle\langle n_{\beta,l}\rangle + \langle c^\dagger_{\alpha,k} c_{\beta,l}\rangle\langle c_{\alpha,l} c^\dagger_{\beta,k}\rangle \cos((k-l)i)) \end{aligned} \tag{A1}$$

in which we assumed $n_{\alpha,j}n_{\beta,j+i} = 1/2n_{\alpha,j}n_{\beta,j+i} + \text{H.c.}$, i.e., any density-density correlator is a real function. The expressions for the interactions of interest are now obtained by using the following single-particle expectation values

$$\langle c^\dagger_{\uparrow,k} c_{\uparrow,k}\rangle = u(k)^2\langle n_{+,k}\rangle + v(k)^2\langle n_{-,k}\rangle, \tag{A2}$$

$$\langle c^\dagger_{\downarrow,k} c_{\downarrow,k}\rangle = v(k)^2\langle n_{+,k}\rangle + u(k)^2\langle n_{-,k}\rangle, \tag{A3}$$

$$\langle c^\dagger_{\uparrow,k} c_{\downarrow,k}\rangle = +u(k)v(k)\langle n_{+,k}\rangle - u(k)v(k)\langle n_{-,k}\rangle. \tag{A4}$$

The interactions considered in the main text are simply given by $\mathcal{H}_U = \mathcal{H}_{\uparrow,\downarrow,0}$, $\mathcal{H}_\parallel = \sum_\alpha \mathcal{H}_{\alpha,\alpha,1}$, and $\mathcal{H}_\parallel = \mathcal{H}_{\uparrow,\downarrow,1} + \mathcal{H}_{\downarrow,\uparrow,1}$. By projection onto the lower band, i.e., $n_{+,k} = 0$, and substituting the expressions in Eqs. (A2)–(A4) for the spinful densities, we find

$$\mathcal{H}_\parallel/2 = \frac{V_\parallel}{L}\sum_{k,l}\left(u_k^2 v_l^2 - u_k^2\left(1 - v_l^2\right)\cos(k-l)\right)\langle n_{-,k}\rangle\langle n_{-,l}\rangle, \tag{A5}$$

$$\mathcal{H}_\perp/2 = \frac{V_\perp}{L}\sum_{k,l}\left(u_k^2 v_l^2 - u_k v_k u_l v_l\cos(k-l))\right)\langle n_{-,k}\rangle\langle n_{-,l}\rangle \tag{A6}$$

$$\mathcal{H}_U = \frac{U}{L}\sum_{k,l}\left(u_k^2 v_l^2 - u_k v_k u_l v_l\right)\langle n_{-,k}\rangle\langle n_{-,l}\rangle. \tag{A7}$$

We use the more convenient form of the coherence factors, which relates their squares to the components of the underlying Hamiltonian's Bloch vector components by the following relations:

$$u_k^2 = \tfrac{1}{2}(1+\tilde{h}_z) \qquad v_k^2 = \tfrac{1}{2}(1-\tilde{h}_z) \qquad 2u_k v_k = \tilde{h}_x. \tag{A8}$$

to arrive at

$$\mathcal{H}_\parallel = \frac{V_\parallel}{2L}\sum_{k,l}(1 + \tilde{h}_z(k)\tilde{h}_z(l) - \tilde{h}_z(k)\tilde{h}_z(l)\cos[k-l])\langle n_{-,k}\rangle\langle n_{-,l}\rangle, \tag{A9}$$

$$\mathcal{H}_\perp = \frac{V_\perp}{2L}\sum_{k,l}(1 - \tilde{h}_z(k)\tilde{h}_z(l) - \tilde{h}_x(k)\tilde{h}_x(l)\cos[k-l])\langle n_{-,k}\rangle\langle n_{-,l}\rangle, \tag{A10}$$

$$\mathcal{H}_U = \frac{U}{4L}\sum_{k,l}(1 - \tilde{h}_z(k)\tilde{h}_z(l) - \tilde{h}_x(k)\tilde{h}_x(l))\langle n_{-,k}\rangle\langle n_{-,l}\rangle. \tag{A11}$$

Coupling with a magnetic field penetrating the ring of atoms is done by introducing a twist $e^{i\Phi}$ in the boundary conditions and, ultimately, results in substituting the arguments in the sums by $k \to k - \Phi/L$ as written in the main text. The final expansion in Φ/L can be done easily by using the following set of equations:

$$\tilde{h}_i(k - \Phi/L) \approx \tilde{h}_i(k) - \frac{\Phi}{L}\tilde{h}_i'(k) + \frac{\Phi^2}{2L^2}\tilde{h}_i''(k), \tag{A12}$$

$$\left(\sum_k \tilde{h}_i(k-\Phi/L)\right)^2 \approx \left(\sum_k \tilde{h}_i(k)\right)^2 + \frac{\Phi^2}{L^2}\left(\left[\sum_k \tilde{h}_i'(k)\right] + \sum_k \tilde{h}_i''(k)\sum_l h_i(l)\right), \tag{A13}$$

$$\sum_{k,l}\tilde{h}_i(k-\Phi/L)\tilde{h}_i(l-\Phi/L)\cos(k-l) \approx \sum_{k,l}\cos(k-l)\left(\tilde{h}_i(k)\tilde{h}_i(l) + \frac{\Phi^2}{L^2}[\tilde{h}_i''(k)\tilde{h}_i(l) + \tilde{h}_i'(k)\tilde{h}_i'(l)]\right), \tag{A14}$$

$$\sum_{k,l}\tilde{h}_x(k-\Phi/L)\tilde{h}_x(l-\Phi/L)\cos(k-l) \approx \left(\sum_k \cos(k)\tilde{h}_x\right)^2 + \frac{\Phi^2}{L^2}\left(\left[\sum_k \sin(k)\tilde{h}_x'(k)\right]^2 + \sum_{k,l}\cos(k)\cos(l)\tilde{h}_x''(k)\tilde{h}_x(l)\right), \tag{A15}$$

$$\sum_{k,l}\tilde{h}_z(k-\Phi/L)\tilde{h}_z(l-\Phi/L)\cos(k-l) \approx \left(\sum_k \sin(k)\tilde{h}_z\right)^2 + \frac{\Phi^2}{L^2}\left(\left[\sum_k \cos(k)\tilde{h}_z'(k)\right]^2 + \sum_{k,l}\sin(k)\sin(l)\tilde{h}_z''(k)\tilde{h}_z(l)\right), \tag{A16}$$

in which we used the fact that odd orders in Φ vanish. Therefore, all the above equations are exact up to $O(\Phi^4)$. Note that in the above, the sums in momentum space are considering all occupied momenta of the bottom band. Finally, the notion of integrals of the Bloch vector components $H_{i,n}^{\alpha,\beta}$ yields the equations discussed in the main text. To visualize the results, we plot the Drude weight shift of each interaction $\mathcal{D}_\parallel/V_\parallel$, $\mathcal{D}_\perp/V_\perp$, and $\mathcal{D}_U/U$ in Fig. 5.

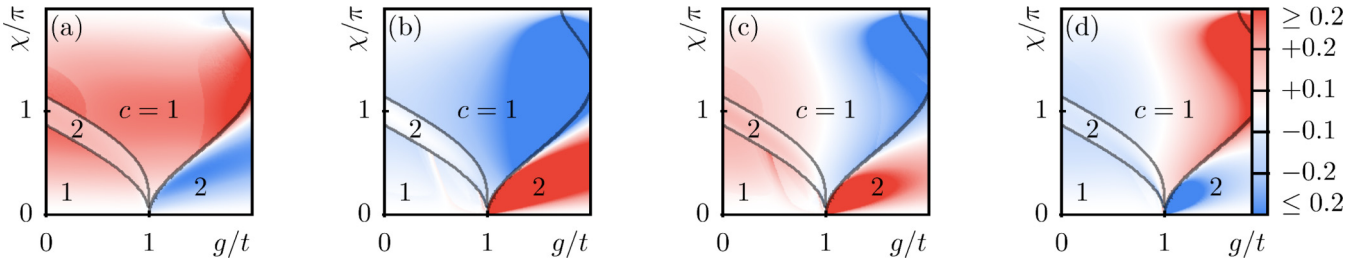

FIG. 5. Change of the Drude weight by interaction according to first-order perturbation theory in the thermodynamic limit for a system at incommensurate total density $n = 20/32$ and $m/t = 1$. (a) $\mathcal{D}_\parallel/V_\parallel$, (b) $\mathcal{D}_\perp/V_\perp$, (c) $\mathcal{D}_\parallel/V_\parallel + \mathcal{D}_\perp/V_\perp$, (d) $\mathcal{D}_U/U$. Solid lines mark the Lifshitz phase transitions between central charge $c = 1$ and $c = 2$. Figure 3 displays cuts of the density plots at $c = 1$ close to $g/t = \chi/\pi = 1$ with markers representing MPS results at $V_\perp/t = 0.1t$, $V_\parallel/t = 0.1t$, and $U/t = 0.125t$.

APPENDIX B: BOSONIZATION: SUPPLEMENTARY

Here we present the detailed derivation of the bosonized Hamiltonian in Eq. (3) of the Creutz model. We begin by projecting the spinors onto left- and right-moving fermions of the bottom band.

$$c_{\uparrow,j} = -e^{ik_F j}v(k_F)R_j - e^{-ik_F j}v(-k_F)L_j, \qquad c_{\downarrow,j} = +e^{ik_F j}u(k_F)R_j + e^{-ik_F j}u(-k_F)L_j. \tag{B1}$$

Next, we insert the projection into the spatial spin densities in the continuum

$$n_\uparrow(x) = v^2(k_F)n_R(x) + v^2(-k_F)n_L(x) + v(-k_F)v(k_F)[e^{-2ik_F x}R^\dagger(x)L(x) + \text{H.c}], \tag{B2}$$

$$n_\downarrow(x) = u^2(k_F)n_R(x) + u^2(-k_F)n_L(x) + u(k_F)u(-k_F)[e^{-2ik_F x}R^\dagger(x)L(x) + \text{H.c.}], \tag{B3}$$

with $x = ja$ and a a dimensional lattice spacing. Next, we plug the densities readily into the expressions of the interactions of interest. One thus finds the effective low-energy expressions according to

$$\begin{aligned}\mathcal{H}_\parallel + \mathcal{H}_\perp = \sum_x [&\gamma_1(n_R(x)n_R(x+a) + n_L(x)n_L(x+a)) + \gamma_2(n_R(x)n_L(x+a) + n_L(x)n_R(x+a)) \\ &+ \gamma_3(e^{2ik_F a}R^\dagger(x)L(x)L^\dagger(x+a)R(x+a) + \text{H.c.})].\end{aligned} \tag{B4}$$

$$\gamma_1 = (u^4 + v^4)V_\parallel + 2u^2v^2V_\perp, \qquad \gamma_2 = 2u^2v^2V_\parallel + (u^4 + v^4)V_\perp, \qquad \gamma_3 = 2u^2v^2(V_\parallel + V_\perp), \tag{B5}$$

in which we used the shorthand notation $u/v = u(k_F)/v(k_F)$. Finally, we find the bosonized Hamiltonian by applying the standard bosonization identities

$$R(x) \sim \frac{1}{\sqrt{2\pi a}}e^{-i(\phi(x)-\theta(x))}, \qquad L(x) \sim \frac{1}{\sqrt{2\pi a}}e^{i(\phi(x)+\theta(x))}, \tag{B6}$$

leading to the bosonization of the point-split operator

$$R^\dagger(x)L(x)L^\dagger(x+a)R(x+a) + \text{H.c.} = -\frac{2\partial_x\phi^2}{(2\pi)^2}, \tag{B7}$$

in which we neglect some infinite, but constant, terms. We notice this expression only involves the density field ϕ. Thus, it does not affect the current operator and has no effect on the Drude weight, even though it affects g_4 and g_2. Finally, we remind that the mover densities relate to the bosonic fields according to

$$n_R(x) = [\partial_x\theta(x) - \partial_x\phi(x)]/2\pi, \qquad n_L(x) = -[\partial_x\theta(x) + \partial_x\phi(x)]/2\pi. \tag{B8}$$

Following this recipe and plugging Eqs. (B8) into Eq. (B4) yields the coupling constants given in Table I, which concludes this Appendix.

APPENDIX C: CROSSOVER TO TWO-DIMENSIONAL SYSTEMS

We generalize the model defined in Sec. III to the case of N legs of the quasi-one-dimensional wire. In momentum space, we choose the transverse flux χ such that the generalized Hamiltonian takes the simple form

$$\begin{aligned}H_0^N(k) = \sum_{j_y} &(m - g\cos k)(c^\dagger_{j_y,k}c_{j_y+1,k} + \text{H.c.}) \\ &- t\cos\big(k - \chi(2j_y - (N+1))\big)n_{j_y,k}.\end{aligned} \tag{C1}$$

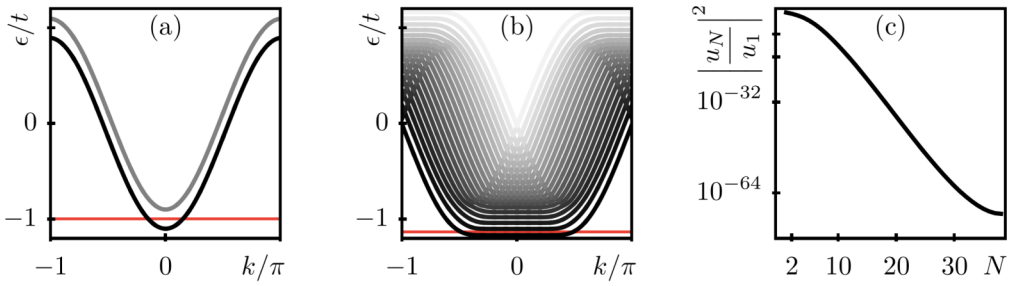

FIG. 6. Coupled-wire approach with (a) $N = 2$ and (b) $N = 20$. We place the Fermi energy in the center of the gap, marked as a red line. In (c), we plot the amplitude $|u_N/u_1(k_F)|^2$ for the case $m = 0.1t$, $g = 0$, and $\chi = 0.025\pi$ versus number of chains N, evidently following an exponential decay. Following Eq. (21) this implies a strong suppression of g_2 processes compared to g_4 in the $c = 1$ gap.

This Hamiltonian may be diagonalized by a rotation onto the bands $U_N(k)$ such that $U_N(k)H_0^N(k)U_N^\dagger(k) = \mathcal{E}_N(k)$, with a diagonal matrix $\mathcal{E}_N(k) = \mathrm{diag}[\varepsilon_1(k), \varepsilon_2(k), \ldots, \varepsilon_N(k)]$ containing the ordered bands $\varepsilon_i(k) \leqslant \varepsilon_{i+1}(k)$ (see Fig. 6). Although more general scenarios may be considered, we focus here on the coupled wire formalism, which is obtained by setting $g = 0$. In particular, this addresses the one-dimensional limit of the Harper-Hofstadter model [100,101], understood as a coupled-wire system [83] and studied recently also in the context of superconductivity [102]. We require a central charge $c = 1$ such that one has a single pair of left- and right-moving species defined on the lowest band $\varepsilon_1(\pm k_F)$. This justifies the approximation similar to Eq. (B1),

$$\begin{pmatrix} c_{1,x} \\ c_{N,x} \end{pmatrix} \sim \begin{pmatrix} u_1(k_F) & u_1(-k_F) \\ u_N(k_F) & u_N(-k_F) \end{pmatrix} \begin{pmatrix} R(x)e^{+ik_F x} \\ L(x)e^{-ik_F x} \end{pmatrix} \tag{C2}$$

with some prefactors u_1 and u_N which depend on the precise form of U_N. A more general form of the imposed interactions in the N-legged setup is

$$\mathcal{H}_\parallel = \sum_{j_x, j_y} V_\parallel(j_y) n_{j_x,j_y} n_{j_x+1,j_y}, \tag{C3}$$

where the local leg density is defined as $n_{j_x,j_y} = c^\dagger_{j_x,j_y} c_{j_x,j_y}$. Due to the nature of the applied projection, other interactions similar to $\mathcal{H}_\perp$ coupling adjacent wires along the y direction will not contribute to the effective model. A hypothetical interaction similar to the two-wire case, which contributes to the projected Hamiltonian is

$$\mathcal{H}_\perp = V_\perp(N) \sum_{j_x} n_{j_x,1} n_{j_x+1,N}. \tag{C4}$$

The remaining calculation to arrive at the Luttinger liquid Hamiltonian is similar to the one presented in main text, and, for $V_\parallel(1) = V_\parallel(N)$ identical g factors are recovered [substituting $u \to u_1$, $v \to u_N$, $V_\parallel \to V_\parallel(1)$, and $V_\perp \to V_\perp(N)$]. As a consequence, the result here is analog to the one presented in the main text

$$g_{4,\parallel} - g_{2,\parallel} = 2\left(u_1^2 - u_N^2\right)^2 > 0. \tag{C5}$$

In Fig. 6 we explicitly target the 2D limit $N \to \infty$, showing that u_1 is the leading contribution, thus strongly suppressing $g_{2,\parallel}$ processes in the effective model. It has to be stressed that Eq. (C2) is not a unitary transformation and projects onto the relevant low-energy sector of the model. In the case of $N > 2$, the bulk is fully projected out in the effective model and only effects on the edges of the system can be recovered. This makes it impossible to deduce bulk properties such as the Hall conductivity σ_H that is instead universally quantized at a given filling. Instead, what we claim here is a strong modification of the edge Drude weight due to interactions for which a universal scaling law dependent on the interactions has been reported using chiral Luttinger liquid approaches [85]. Building up on this statement, we provide here a generic example that enhancement effects of the Drude weight become universally applicable for systems hosting polarized conduction bands dressed with repulsive density-density interactions.

APPENDIX D: COMPARISON BETWEEN LEADING-ORDER PERTURBATION THEORY AND BOSONIZATION

Major deviations between perturbation theory and bosonization arise from Eq. (B1), which requires a flat rotation matrix U. In particular, according to first-order perturbation theory, the canonical operators can be expressed using the bottom band modes only, i.e.,

$$\begin{aligned} c_{\uparrow,j} = {} & e^{ik_F x} v(k_F) \sum_q e^{iqx} \left(1 + \sum_{n=1}^{\infty} \frac{q^n}{n!} \frac{v^{(n)}}{v}(k_F)\right) d_{-,q+k_F} \\ & + e^{-ik_F x} v(-k_F) \sum_q e^{iqx} \left(1 + \sum_{n=1}^{\infty} \frac{q^n}{n!} \frac{v^{(n)}}{v}(-k_F)\right) d_{-,q-k_F} \end{aligned} \tag{D1}$$

and a similar expression ($v \leftrightarrow u$) holds for the down species. To arrive at Eq. (B1), we assume flat coherence factors

$$\sum_{n=1}^{\infty} \frac{q^n}{n!} \frac{f^{(n)}}{f}(\pm k_F) \approx 0, \quad f \in \{u, v\}. \tag{D2}$$

The momentum transfer in forward-scattering processes g_4 is small compared to the Fermi momentum and the above equation is automatically satisfied. However, back-scattering processes g_2 always transfer momentum comparable to k_F and the above equation requires the rotation matrix being almost constant in q, i.e., $U^{(n)}/U(q) \approx 0$. We show a few example contours of the first three derivatives of $|f^{(n)}/f(k_F)|$ along g and χ in Fig. 7, which indeed explains major deviations at regions in which $u^{(n)}/u$ and $v^{(n)}/v$ are large.

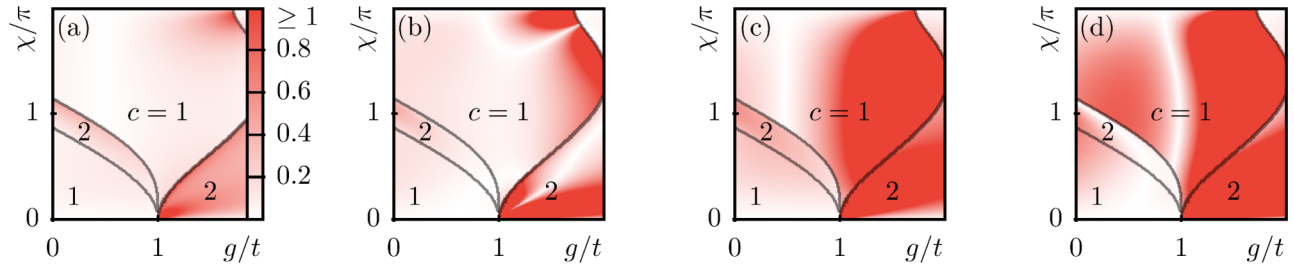

FIG. 7. (a)–(b) First two derivatives of $|u^{(n)}/u(k_F)|$, (c)–(d) first two derivatives of $|v^{(n)}/v(k_F)|$ versus g and flux χ at density $n = 2/3$ and $m = 1$. Discrepancies between bosonization and perturbation theory arise due to a strong violation of Eq. (D2).

On the contrary, at the single Dirac cone point $g = \chi/\pi = 1$ the rotation matrix has entries $u/v(k) = \cos / \sin(k/4)$, as a consequence the n'th derivatives are exponentially suppressed in n and Eq. (D2) becomes a reasonable approximation. Clearly, in regions outside of Eq. (D2), g_2 processes are not correctly considered in the effective model and thus strong deviations in $\mathcal{D}_\perp$ are expected. Remarkably, the qualitative predictions of the effective model extend to the full $c = 1$ region, i.e., we find a positive shift of the Drude weight induced by $\mathcal{H}_\parallel$, and a negative effect of comparable amplitude due to $\mathcal{H}_\perp$.

In conclusion, the above equation fully disregards band and coherence factor curvature, yielding a consistent result with leading-order perturbation theory up to zeroth order in the coherence factor derivatives only [$H^{0,0}_{z,1} = 2\tilde{h}_z(k_F)$ terms in the Drude weights are recovered]. For a future investigation, it is interesting to relax Eq. (D2), in particular keeping more and more higher-order terms in q. This not only accounts for a sum of right and left movers on different lattice sites in Eq. (B1), it naturally reintroduces nontrivial curvature of the coherence factors $u(k)$ and $v(k)$, ultimately giving subleading corrections to γ_i in Eq. (B4).

APPENDIX E: DETAILS ON THE MPS SIMULATIONS

The matrix product states (MPS) results presented in the main text were performed by our own implementation of a U(1) symmetric code preserving the total number of particles, based on the anthology of tensor networks build on a symmetry-preserving library in collaboration with the group of S. Montangero at the University of Ulm [103]. Periodic boundary conditions (PBC) in general are hard to tackle using tensor network schemes due to the absence of a canonical form, which is a necessity to simplify the computational complexity in variational optimizations [104]. A naive solution used heavily in exact diagonalization is the introduction of long-range terms mimicking periodic boundary conditions by coupling the edges of the system. However, such a strategy is deemed to fail for MPS ansätze because, by construction, long-range correlations are not captured sufficiently. An alternative scheme is obtained by deforming the ring into a 1D open boundary system with short-range next-to-nearest-neighbor couplings, depicted in Fig. 8(a). This deformation amends the strong asymmetry between short-range hoppings and long-range boundary terms by reshuffling the lattice sites. The two depicted ring geometries are numerically equivalent and yield an efficient simulation of periodic boundary conditions with open boundary MPS algorithms at the cost of slightly increasing the matrix product operator (MPO) dimension.

The extraction of the particle mobility $\mathcal{D}$ is straightforward; we simulated the ground-state energy dependence $E(\Phi)$ on the magnetic flux Φ penetrating the ring. Numerically, coupling to a magnetic flux is readily done by applying the local transformations $t \to te^{i\Phi/L}$ and $g \to ge^{i\Phi/L}$ in the real-space kinetic Hamiltonian $\mathcal{H}_{\text{kin}}$. The susceptibility function can then be extracted by two equivalent procedures: (i) by approximating the second derivative according to

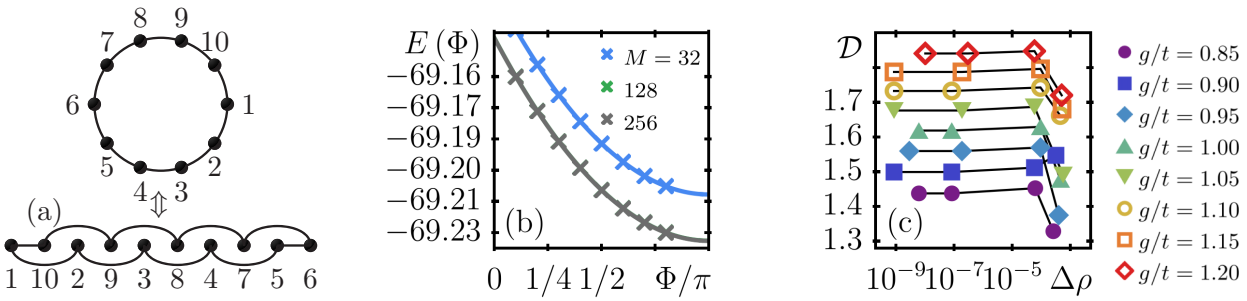

FIG. 8. (a) Deformation of a generic ring system to simulate periodic boundary conditions with open boundary MPS algorithms. (b) Generic representative of numerical simulations with different bond dimension M of the ground-state energy dependence $E(\Phi)$ for a system at fixed density $n = N/L = 20/32$ at parameters $m/t = \chi/\pi = 1$, $g/t = 1.2$, $U/t = 4$, and $V_\parallel = V_\perp = 0$. Crosses represent MPS results and continuous lines represent a quadratic fit. At the presented decimal precision, data and fits for $M = 128$ and $M = 256$ reside exactly on top of each other. (c) Dependence of the Drude weight on the truncated probability $\Delta\rho$ of the MPS. In case of $\Delta\rho < 10^{-7}$, the data is sufficiently converged up to the necessary precision presented in the main text and the convergence error may be disregarded.

$\partial_\Phi^2 E(\Phi) = [E(\Phi+\epsilon) + E(\Phi-\epsilon) - 2E(\Phi)]/\epsilon^2 + O(\epsilon^4)$, sending $\epsilon \to 0$ and then $\Phi \to \Phi_m$, or by (ii) fitting the energy dependence. Hereby, Φ_m is the energy extremum, which depends on the parity of the underlying system. In most cases, $\Phi_m = 0/\pi$ for an odd/even number of fermions, respectively [105]. According to leading-order perturbation theory, it is possible to extract the mobility $\mathcal{D}$ by a quadratic fit function f to approximate the energy dependence $E(\Phi)$ according to $f(\Phi) = a + b(\Phi - \Phi_m)^2$ with Φ_m being the energy extremum, and the Drude weight being $\mathcal{D} = 2\pi L b$, which is correct up to $O[(\Phi - \Phi_m)^4]$ in the flux Φ. Due to an astonishing agreement between prediction and numerics, even for strong interaction amplitudes, we present a generic representative of the fitting procedure in Fig. 8(b). A basic estimation of the numerical accuracy is governed by Fig. 8(c), in which we display the convergence of the presented observables versus $\Delta\rho$, the figure of merit in MPS simulations representing the truncated probability of the reduced density matrix for the canonical bipartition at the center of the chain.

[1] W. Kohn, Phys. Rev. **133**, A171 (1964).
[2] B. S. Shastry and B. Sutherland, Phys. Rev. Lett. **65**, 243 (1990).
[3] R. M. Fye, M. J. Martins, D. J. Scalapino, J. Wagner, and W. Hanke, Phys. Rev. B **44**, 6909 (1991).
[4] D. J. Scalapino, S. R. White, and S. C. Zhang, Phys. Rev. Lett. **68**, 2830 (1992).
[5] T. Giamarchi and B. S. Shastry, Phys. Rev. B **51**, 10915 (1995).
[6] M. Büttiker, Y. Imry, and R. Landauer, Phys. Lett. A **96**, 365 (1983).
[7] H.-F. Cheung, E. K. Riedel, and Y. Gefen, Phys. Rev. Lett. **62**, 587 (1989).
[8] L. P. Lévy, G. Dolan, J. Dunsmuir, and H. Bouchiat, Phys. Rev. Lett. **64**, 2074 (1990).
[9] A. C. Bleszynski-Jayich, W. E. Shanks, B. Peaudecerf, E. Ginossar, F. V. Oppen, L. Glazman, and J. G. E. Harris, Science **326**, 272 (2009).
[10] I. O. Kulik, Low Temp. Phys. **36**, 841 (2010).
[11] S. Viefers, P. Koskinen, P. Singha Deo, and M. Manninen, Phys. E: Low-dimensional Syst. Nanostruct. **21**, 1 (2004).
[12] A. Schmid, Phys. Rev. Lett. **66**, 80 (1991); V. Ambegaokar and U. Eckern, *ibid.* **67**, 3192 (1991).
[13] H. Bary-Soroker, O. Entin-Wohlman, and Y. Imry, Phys. Rev. Lett. **101**, 057001 (2008).
[14] H. Bouchiat, Physics **1**, 7 (2008).
[15] D. J. Thouless, Phys. Rep. **13**, 93 (1974).
[16] J. T. Edwards and D. J. Thouless, J. Phys. C: Solid State Phys. **5**, 807 (1972).
[17] E. Abrahams, P. W. Anderson, D. C. Licciardello, and T. V. Ramakrishnan, Phys. Rev. Lett. **42**, 673 (1979).
[18] E. Akkermans and G. Montambaux, Phys. Rev. Lett. **68**, 642 (1992).
[19] G. Bouzerar, D. Poilblanc, and G. Montambaux, Phys. Rev. B **49**, 8258 (1994).
[20] F. von Oppen, Phys. Rev. Lett. **73**, 798 (1994).
[21] F. von Oppen, Phys. Rev. E **51**, 2647 (1995).
[22] M. Filippone, P. W. Brouwer, J. Eisert, and F. von Oppen, Phys. Rev. B **94**, 201112(R) (2016).
[23] T. Giamarchi and A. J. Millis, Phys. Rev. B **46**, 9325 (1992).
[24] H. Castella, X. Zotos, and P. Prelovšek, Phys. Rev. Lett. **74**, 972 (1995).
[25] X. Zotos and P. Prelovšek, Phys. Rev. B **53**, 983 (1996).
[26] B. N. Narozhny, Phys. Rev. B **54**, 3311 (1996).
[27] B. N. Narozhny, A. J. Millis, and N. Andrei, Phys. Rev. B **58**, R2921 (1998).
[28] K. Fabricius and B. M. McCoy, Phys. Rev. B **57**, 8340 (1998).
[29] X. Zotos, Phys. Rev. Lett. **82**, 1764 (1999).
[30] A. Rosch and N. Andrei, Phys. Rev. Lett. **85**, 1092 (2000).
[31] F. Heidrich-Meisner, A. Honecker, D. C. Cabra, and W. Brenig, Phys. Rev. B **68**, 134436 (2003).
[32] T. Prosen, Phys. Rev. Lett. **106**, 217206 (2011).
[33] C. Karrasch, J. H. Bardarson, and J. E. Moore, Phys. Rev. Lett. **108**, 227206 (2012).
[34] C. Karrasch, D. M. Kennes, and F. Heidrich-Meisner, Phys. Rev. B **91**, 115130 (2015).
[35] R. Steinigeweg, J. Herbrych, F. Pollmann, and W. Brenig, Phys. Rev. B **94**, 180401(R) (2016).
[36] M. Ljubotina, M. Žnidarič, and T. Prosen, Nature Commun. **8**, 16117 (2017).
[37] M. Steiner, J. Villain, and C. Windsor, Adv. Phys. **25**, 87 (1976).
[38] T. Ami, M. K. Crawford, R. L. Harlow, Z. R. Wang, D. C. Johnston, Q. Huang, and R. W. Erwin, Phys. Rev. B **51**, 5994 (1995).
[39] M. Takigawa, T. Asano, Y. Ajiro, M. Mekata, and Y. J. Uemura, Phys. Rev. Lett. **76**, 2173 (1996).
[40] M. Takigawa, N. Motoyama, H. Eisaki, and S. Uchida, Phys. Rev. Lett. **76**, 4612 (1996).
[41] A. V. Sologubenko, E. Felder, K. Giannò, H. R. Ott, A. Vietkine, and A. Revcolevschi, Phys. Rev. B **62**, R6108(R) (2000).
[42] A. V. Sologubenko, K. Giannò, H. R. Ott, A. Vietkine, and A. Revcolevschi, Phys. Rev. B **64**, 054412 (2001).
[43] K. R. Thurber, A. W. Hunt, T. Imai, and F. C. Chou, Phys. Rev. Lett. **87**, 247202 (2001).
[44] F. L. Pratt, S. J. Blundell, T. Lancaster, C. Baines, and S. Takagi, Phys. Rev. Lett. **96**, 247203 (2006).
[45] X. Zotos, F. Naef, M. Long, and P. Prelovšek, Phys. Rev. Lett. **85**, 377 (2000).
[46] S. Greschner, M. Filippone, and T. Giamarchi, Phys. Rev. Lett. **122**, 083402 (2019).
[47] J. A. Sauer, M. D. Barrett, and M. S. Chapman, Phys. Rev. Lett. **87**, 270401 (2001).
[48] S. Gupta, K. W. Murch, K. L. Moore, T. P. Purdy, and D. M. Stamper-Kurn, Phys. Rev. Lett. **95**, 143201 (2005).
[49] C. Ryu, M. F. Andersen, P. Cladé, V. Natarajan, K. Helmerson, and W. D. Phillips, Phys. Rev. Lett. **99**, 260401 (2007).
[50] I. Lesanovsky and W. von Klitzing, Phys. Rev. Lett. **99**, 083001 (2007).
[51] S. Eckel, F. Jendrzejewski, A. Kumar, C. J. Lobb, and G. K. Campbell, Phys. Rev. X **4**, 031052 (2014).

[52] M. Łącki, H. Pichler, A. Sterdyniak, A. Lyras, V. E. Lembessis, O. Al-Dossary, J. C. Budich, and P. Zoller, Phys. Rev. A **93**, 013604 (2016).

[53] L. Amico, A. Osterloh, and F. Cataliotti, Phys. Rev. Lett. **95**, 063201 (2005).

[54] M. Cominotti, D. Rossini, M. Rizzi, F. Hekking, and A. Minguzzi, Phys. Rev. Lett. **113**, 025301 (2014).

[55] A. Gallemí, M. Guilleumas, M. Richard, and A. Minguzzi, Phys. Rev. B **98**, 104502 (2018).

[56] M. Mancini, G. Pagano, G. Cappellini, L. Livi, M. Rider, J. Catani, C. Sias, P. Zoller, M. Inguscio, M. Dalmonte, and L. Fallani, Science **349**, 1510 (2015).

[57] D. Genkina, L. M. Aycock, H.-I. Lu, M. Lu, A. M. Pineiro, and I. B. Spielman, New J. Phys. **21**, 053021 (2019).

[58] F. C. Dias, I. R. Pimentel, and M. Henkel, Phys. Rev. B **73**, 075109 (2006).

[59] V. Meden and U. Schollwöck, Phys. Rev. B **67**, 035106 (2003).

[60] R. Berkovits, Phys. Rev. B **48**, 14381 (1993).

[61] M. Bischoff, J. Jünemann, M. Polini, and M. Rizzi, Phys. Rev. B **96**, 241112(R) (2017).

[62] A. Principi, M. Polini, G. Vignale, and M. I. Katsnelson, Phys. Rev. Lett. **104**, 225503 (2010).

[63] B. A. Bernevig and T. L. Hughes, *Topological Insulators and Topological Superconductors* (Princeton University Press, Princeton, 2013).

[64] T. Giamarchi, *Quantum Physics in One Dimension*, Vol. 121 (Oxford University Press, New York, 2004).

[65] J. v. Delft and H. Schoeller, Ann. Phys. (NY) **7**, 225 (1998).

[66] G. Dresselhaus, Phys. Rev. **100**, 580 (1955).

[67] A. Haller, M. Rizzi, and M. Burrello, New J. Phys. **20**, 053007 (2018).

[68] F. Mireles and G. Kirczenow, Phys. Rev. B **64**, 024426 (2001).

[69] D. Frustaglia and K. Richter, Phys. Rev. B **69**, 235310 (2004).

[70] T. Ozawa and H. M. Price, Nature Rev. Phys. **1**, 349 (2019).

[71] U. Ledermann and K. Le Hur, Phys. Rev. B **61**, 2497 (2000).

[72] A. E. Feiguin and F. Heidrich-Meisner, Phys. Rev. Lett. **102**, 076403 (2009).

[73] A. Petrescu and K. Le Hur, Phys. Rev. B **91**, 054520 (2015).

[74] E. Cornfeld and E. Sela, Phys. Rev. B **92**, 115446 (2015).

[75] S. Greschner, M. Piraud, F. Heidrich-Meisner, I. P. McCulloch, U. Schollwöck, and T. Vekua, Phys. Rev. A **94**, 063628 (2016).

[76] M. Calvanese Strinati, E. Cornfeld, D. Rossini, S. Barbarino, M. Dalmonte, R. Fazio, E. Sela, and L. Mazza, Phys. Rev. X **7**, 021033 (2017).

[77] A. Petrescu, M. Piraud, G. Roux, I. P. McCulloch, and K. Le Hur, Phys. Rev. B **96**, 014524 (2017).

[78] M. Creutz, Phys. Rev. Lett. **83**, 2636 (1999).

[79] J. Jünemann, A. Piga, S.-J. Ran, M. Lewenstein, M. Rizzi, and A. Bermudez, Phys. Rev. X **7**, 031057 (2017).

[80] S. T. Carr, B. N. Narozhny, and A. A. Nersesyan, Ann. Phys. (NY) **339**, 22 (2013).

[81] B. N. Narozhny, S. T. Carr, and A. A. Nersesyan, Phys. Rev. B **71**, 161101(R) (2005).

[82] S. T. Carr, B. N. Narozhny, and A. A. Nersesyan, Phys. Rev. B **73**, 195114 (2006).

[83] C. L. Kane, R. Mukhopadhyay, and T. C. Lubensky, Phys. Rev. Lett. **88**, 036401 (2002).

[84] T. Meng, Eur. Phys. J. Special Topics **229**, 527 (2020).

[85] G. Antinucci, V. Mastropietro, and M. Porta, Commun. Math. Phys. **362**, 295 (2018).

[86] X. G. Wen, Phys. Rev. B **41**, 12838 (1990).

[87] L. Del Re and M. Capone, Phys. Rev. A **98**, 063628 (2018).

[88] B. Hetényi, Phys. Rev. B **87**, 235123 (2013).

[89] D. Sticlet, B. Dóra, and J. Cayssol, Phys. Rev. B **88**, 205401 (2013).

[90] J.-P. Brantut, C. Grenier, J. Meineke, D. Stadler, S. Krinner, C. Kollath, T. Esslinger, and A. Georges, Science **342**, 713 (2013).

[91] S. Krinner, D. Stadler, D. Husmann, J.-P. Brantut, and T. Esslinger, Nature (London) **517**, 64 (2014).

[92] M. Lebrat, P. Grišins, D. Husmann, S. Häusler, L. Corman, T. Giamarchi, J.-P. Brantut, and T. Esslinger, Phys. Rev. X **8**, 011053 (2018).

[93] D. J. Papoular, L. P. Pitaevskii, and S. Stringari, Phys. Rev. Lett. **113**, 170601 (2014).

[94] M. Filippone, F. Hekking, and A. Minguzzi, Phys. Rev. A **93**, 011602(R) (2016).

[95] D. P. Simpson, D. M. Gangardt, I. V. Lerner, and P. Krüger, Phys. Rev. Lett. **112**, 100601 (2014).

[96] D. L. Maslov and M. Stone, Phys. Rev. B **52**, R5539(R) (1995); I. Safi and H. J. Schulz, *ibid.* **52**, R17040(R) (1995). V. V. Ponomarenko, *ibid.* **52**, R8666(R) (1995).

[97] G. Salerno, H. M. Price, M. Lebrat, S. Häusler, T. Esslinger, L. Corman, J.-P. Brantut, and N. Goldman, Phys. Rev. X **9**, 041001 (2019).

[98] M. Filippone, C.-E. Bardyn, S. Greschner, and T. Giamarchi, Phys. Rev. Lett. **123**, 086803 (2019).

[99] M. Calvanese Strinati, S. Sahoo, K. Shtengel, and E. Sela, Phys. Rev. B **99**, 245101 (2019).

[100] P. G. Harper, Proc. Phys. Soc. A **68**, 874 (1955).

[101] D. R. Hofstadter, Phys. Rev. B **14**, 2239 (1976).

[102] F. Yang, V. Perrin, A. Petrescu, I. Garate, and K. Le Hur, Phys. Rev. B **101**, 085116 (2020).

[103] P. Silvi, F. Tschirsich, M. Gerster, J. Jünemann, D. Jaschke, M. Rizzi, and S. Montangero, Sci. Post. Phys. Lect. Notes, 8 (2019).

[104] U. Schollwöck, Ann. Phys. (NY) **326**, 96 (2011).

[105] M. Filippone, C.-E. Bardyn, and T. Giamarchi, Phys. Rev. B **97**, 201408(R) (2018).